Translated from *Uspekhi Khimii*, **55**, 608-636 (1986) U.D.C. 538.736

Diffraction Methods for the Investigation of the Electron Density and Dynamics of Crystal Lattices

V.G.Tsirel'son, Yu.Z.Nozik, and V.S.Urusov

Precision diffraction methods for the investigation of the electron density, electrostatic potential, and dynamics of crystal lattices are described. Data concerning the fine details of the chemical bonds in compounds of various classes obtained with their aid are discussed. The forms in which the data on the distribution of electron density and electrostatic potential in crystals can be represented and interpreted are examined.
The bibliography includes 96 references.

CONTENTS

I. Introduction 316
II. Experimental study of the distribution of electron density 316
III. Methods for the representation of electron density 320
IV. The electrostatic field in the crystal 325
V. The atomic (one-particle) potentials 326
VI. Characteristics of the electronic structure of crystals of different types 326

I. INTRODUCTION

Two approaches to the description of the structures of molecules and crystals have arisen hitherto. The first of these, namely the quantum-chemical approach, reduces to seeking (in terms of a particular type of approximation) the solution to the Schrödinger equation and their chemical interpretation constitutes an exceptionally difficult problem. In the other, crystal-chemical approach, the structure of the substance is described on the basis of a simple geometrical model and the concepts of the effective charges and radii of atoms.

The two approaches have now come together to some extent owing to factors dictated by practical chemical problems. Qualitatively, the new level of these problems required a fairly rigorous description of the structure and detailed properties of crystals with a complex structure of chemical bonds. Such a description has been achieved by introducing the function $\rho(\mathbf{r})$ characterising the total electron density in the molecule or crystal. This function contains an appreciable proportion of the chemical information about the system, can be related to chemical concepts, can be visualised by graphical representation, and finally its values can be measured directly by X-ray diffraction. The last factor is of fundamental importance because, instead of abstract parameters, determined by wave functions, it makes it possible to describe the electronic structure of the substance with the aid of the experimental function $\rho(\mathbf{r})$.

Together with a brief description of the modern methods for the interpretation of diffraction data and the estimation of their accuracy, the aim of the present review is to demonstrate for a series of examples in what way the results obtained with the aid of precision X-ray measurements can be interpreted in terms of the language of quantum chemistry and crystal chemistry. It is particularly important that the data obtained by this method concern complex chemical compounds which are not susceptible to modern quantum-chemical computational methods.

The use of diffraction methods normally reduces to the determination of the coordinates and parameters of the thermal vibrations of atoms in the crystal lattice. However, by virtue of the significant increase in accuracy of structural analysis as a result of the wide-scale introduction of automatic diffractometers and the development of methods for the accurate interpretation of experimental data, detailed investigation of charge distribution and potential near the equilibrium positions of the atoms in crystals has become possible in recent years. The application of the neutron diffraction method in addition to X-ray data has significantly expanded the range of information obtained.

The qualitative imporvement of the apparatus for the diffraction methods has entailed a change in all the stages of the experiment and of the treatment of the results of measurements. We therefore thought it useful to describe concisely all the stages of the accurate measurement and interpretation of diffraction data. The expansion of experimental possibilities has sharply increased the number of studies based on diffraction methods. They have been devoted to the experimental refinement of the traditional ideas of structural chemistry and the theoretical interpretation of the data obtained. These questions, together with the description of the principles of the precision X-ray and neutron diffraction methods and the analysis of the accuracy of the results, the methods of their representation, and their comparison with data derived by quantum-chemical calculations, are examined in this review. The review does not deal with questions of the determination of spin and momentum densities by diffraction methods in molecules and crystals, which have been considered in detail in a collected volume.[1]

II. EXPERIMENTAL STUDY OF THE DISTRIBUTION OF ELECTRON DENSITY

In terms of the adiabatic approximation,[2] it is possible to separate with adequate accuracy the movements of electrons and nuclei and to examine the electron subsystem for the nuclear configuration fixed by the thermal equilibrium positions. The structure and properties of the N-electron subsystem in the ground state are then described by the many-electron wave function $\Psi(\mathbf{x}_1, \ldots, \mathbf{x}_N)$, which depends on the three-dimensional coordinates and spins of all the electrons. This function can be found as the solution of the Schrödinger equation on the basis of the variational principle. This mathematically cumbersome procedure yields results which depend on the level of the approximations adopted and on the quality of the basis functions used.

For this reason, it is exceptionally difficult to obtain the complete wave function Ψ which reproduces correctly all the properties of the many-electron system;[3] furthermore, the practical determination of such characteristics from Ψ is fairly difficult. However, it is possible to use for the description of the majority of the physicochemical properties of molecules and crystals a one-electron density distribution function $\rho(\mathbf{r})$ with a simpler structure, the function depending solely on the three-dimensional coordinates of the point at which the charge density is to be determined. This function is related to Ψ by the expression[2]

$$\rho(\mathbf{r}) = N \int \ldots \int \Psi(\mathbf{x}_1, \ldots, \mathbf{x}_N) \cdot \Psi^*(\mathbf{x}_1, \ldots, \mathbf{x}_N)\, d\mathbf{x}_2 \ldots d\mathbf{x}_N d\mathbf{s}_1, \qquad (1)$$

where $\mathbf{x}_i = \mathbf{r}_i \mathbf{s}_i$, $\mathbf{r}_i$ being the three-dimensional coordinates, $\mathbf{s}_i$ the spin coordinates of the ith electron, and N the number of electrons in the system.

The theoretical interpretation of the function ρ is significantly simpler than that of the wave function Ψ and Eqn.(1) makes it possible to determine it.

The wave function Ψ (with its numerical characteristics) can be calculated with the aid of one of the approximate versions of the solution of the Shcrödinger equation, for example, by the self-consistent field method in terms of the Hartree–Fock approximation, the configuration interaction method, and also the methods based on the band theory of solids. However, the problem of the correct description of the electron density distribution at all points in the test system is very difficult and such description has been achieved (with an error of approximately 0.1 $e\text{Å}^{-3}$) only for simple 2–6 atom molecules.[4,5] For more complex many-electron systems and especially for crystals, the realistically attainable accuracy of the theoretical calculations of electron density is to within approximately 0.3 $e\text{Å}^{-3}$, which is clearly inadequate for the solution of many chemical problems.

On the other hand, the function ρ can be measured experimentally because elastic (Bragg) X-ray scattering by the crystal entails the interaction of the radiation with the electrons and the signal contains information about their distributions. Having measured the intensities of the X-ray reflections for various atomic planes with the *hkl* indices, it is possible to obtain the time-average electron density function† at any point with the coordinates *xyz* in a unit cell having the volume V (Vainshtein[6]):

$$\rho(\mathbf{r}) \equiv \rho(xyz) = \frac{1}{V} \sum_{hkl} F(hkl) \exp[-2\pi i(hx + ky + lz)] \qquad (2)$$

where $F(hkl)$ is the structural amplitude related to the reflection intensity measured in the X-ray diffraction experiment. Thus Eqn.(2) makes it possible to determine directly the electron density distribution in the crystal (Fig.1). The accuracy of the determination of ρ depends on a number of factors and will be examined in detail below. Here we shall only note that in many instances the error can be only 0.02 $e\text{Å}^{-3}$.

The classical X-ray diffraction analysis of structure is based on the hypothesis that the maxima in the function ρ correspond to the centres of gravity in the electron densities of the atoms; approximate values of these maxima can be found by special methods.[6] The coordinates of the atoms and the parameters of their anisotropic vibrations are then refined by the method of least squares based on minimising the functional

$$\Phi = \sum_{hkl} [F(hkl) - F_{\text{calc}}(hkl)]^2. \qquad (3)$$

The model of the structure to be refined is specified by the expression for the structural amplitude:

$$F_{\text{calc}}(hkl) = \sum_{n=1}^{m} f_n W_n(hkl) \exp[2\pi i(hx + ky + lz)],$$

where the atomic amplitude f_n describes the scattering capacity of the nth atom with the coordinates x_n, y_n, and z_n and the temperature multiplier W_n takes into account the thermal parameters.

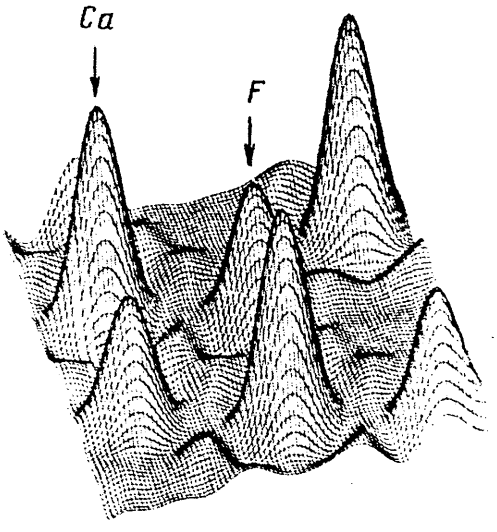


Figure 1. The map of the total electron density in the CaF_2 crystals; the maxima of the ρ function correspond to the positions of the atoms.

The atomic amplitude f_n is related by the Fourier transformation to the function of the static electron density of the atom. For an atom in the crystal, this function is never known accurately; to a first approximation, it is assumed that a crystal made up of spherically symmetrical atoms constitutes a satisfactory *a priori* model. This made it possible to describe and tabulate the values of f for all atoms on the basis of the calculation of their spherically symmetrical electron densities by quantum-chemical methods; these f curves are in fact normally used in practice.[7] The errors of their calculation are less than 0.5% (somewhat more for heavy atoms). However, one should note that the above error is not a criterion of the suitability of the spherical atom model for the refinement by the method of least squares. In fact, the modification of the atomic electron density through chemical interaction disturbs the spherical symmetry of the atom and leads to a dependence of the atomic amplitude on the direction of scattering of X-rays. The structural parameters found within the framework of the traditional approach can therefore contain errors associated with this factor.

†The averaging arises because the measurement takes place over a period of time.

In order to take into account the thermal movement of the crystals, one uses the approximation according to which the electron density ρ "smeared" by the atomic vibrations is represented by the convolution of the theoretical static density and the distribution function $t(\mathbf{R})$ for the positions of the centres of gravity of the vibrating atoms $\mathbf{R}$.[8] For an individual atom, this can be formulated as follows:

$$\rho_n(\mathbf{r}) = \int \rho_n(\mathbf{r}, \mathbf{R})\, t_n(\mathbf{R})\, d\mathbf{R}. \quad (5)$$

The specific form of the function t_n depends on the characteristics of the crystal field potential near the point of thermal equilibrium of the atom. In early studies, this potential was assumed to be harmonic and the function was represented by a three-dimensional Gaussian distribution function. However, in a real case the atomic vibrations are anharmonic and the anharmonicity parameters can be determined experimentally, which is done by introducing additional terms into the t_n refined by the method of least squares.[8] An example of such a description is provided by the cumulative expansion of this function when the temperature multiplier assumes the form[6]

$$W_n = \overline{\exp}\left[-\sum_{ij}\beta^{ij}h_ih_k - \sum_{ijk}\gamma^{ijk}h_ih_jh_k + \sum_{ijkl}\delta^{ijkl}h_ih_jh_kh_l + \ldots\right], \quad (6)$$

where β^{ij}, γ^{ijk}, and δ^{ijkl} are the elements of the tensors describing the harmonic and anharmonic (third- and fourth-order) thermal vibrations of the atoms and the h's are the Miller indices. Other expansions of the functions t_n can also be encountered.[8]

A relation of type (2) can be obtained likewise for the distribution of nuclear density; in this case the structural amplitudes $f(hkl)$ are measured in a neutron diffraction experiment and the maxima of the density function correspond to the centres of gravity of the ellipsoids of the thermal vibrations of the nuclei. Owing to the small dimensions of the nuclei, the neutron scattering by the atom is spherically symmetrical. The amplitude of the coherent scattering of neutrons b_n is determined by the properties of the given nucleus and, in contrast to the atomic amplitude f_n, is independent of both the magnitude and direction of the scattering vector, i.e. $b_n = \text{const}$.[9]

In terms of the adiabatic approximation, the parameters of the thermal vibrations of the atomic nuclei and of their electron shells are identical. In terms of this approximation, one can assume that the information obtained by the X-ray and neutron diffraction methods (taking into account their specific features—see below) is identical. However, one should note that at the present time the data produced by accurate diffraction experiments show that in certain cases the use of the adiabatic approximation is inadmissible; for example, highly delocalised valence electrons and conductivity electrons do not obey this approximation. On the other hand, if this approximation is adopted, then certain inaccuracies, mentioned above, in the determination of the structural parameters from X-ray data owing to the non-spherical nature of the electron density of the atoms can be eliminated in the subsequent analysis of the electron distribution. The analogous parameters obtained from neutron diffraction measurements can be used instead of the X-ray parameters.

The joint application of various diffraction methods can be generally speaking extremely useful. For example, the scattering of electrons is determined by the electrostatic potential of the atom, which depends on the charge distribution in the crystal. We have the relation[6] between the amplitude of the scattering of electrons and X-rays:

$$f_{el}[(\sin\theta)/\lambda)] = \frac{8\pi^2me^2}{h^2}\cdot\frac{Z - f_p[(\sin\theta)/\lambda]}{[(\sin\theta)/\lambda]^2}, \quad (7)$$

where h is the Planck constant, e and m are the charge and mass of the electron, and Z is the atomic charge. Using the values on the X-ray f curves refined on the basis of experimental data (see below), it is possible to calculate f_{el} more accurately by Eqn.(7), which permits an improvement of the accuracy of the structural information.

In order to make use of the information derived from the diffraction experiments in the study of electron density, it is essential to relate ρ directly to the measured radiation intensity. This can be done within the framework of the kinematic theory of diffraction taking into account the corresponding dynamic corrections.[6,9] If the homogeneous monochromatic X-ray beam is incident on a crystal, then the total measured intensity of the scattered radiation can be formulated as follows:

$$T(\mathbf{q}) = JK(e^2/mc^2V)^2v\lambda^3LP(1+\alpha)\cdot|yDF(\mathbf{q})|^2 + \sum_m p_mI_m(\mathbf{q}) + B, \quad (8)$$

where $\mathbf{q}$ is a vector whose coordinates are the Miller indices, h, k, and l [it is the scattering vector $|\mathbf{q}| = 4\pi(\sin\theta)/\lambda$], K a multiplier which takes into account the drift of the primary beam over a long period, $A(\mu)$ the transmission function which depends on the absorption coefficient μ, α a correction for the thermal diffuse scattering, V the volume of the unit cell, B the background intensity, p_m are coefficients taking into account the energy exchange between the incident and reflected beams with the intensities I_m under the conditions of repeated scattering, J is the intensity of the incident radiation with a wavelength λ per unit area, e^2/mc^2 the electron multiplier, v the volume of the crystal involved in the reflection, P the polarisation multiplier, L the Lorentz factor, y the correction for extinction, and D the correction for anomalous scattering.[6]

The formula for the intensities of neutron diffraction can be formulated analogously.[9] In this case the multiplier e^2/mc^2 is omitted from Eqn.(2) and, in view of the lack of polarisation of the neutrons, $P = 1$.

Eqn.(8) can be conveniently rewritten in the form

$$T(\mathbf{q}) = I(\mathbf{q})/M + \sum_m p_mI_m(\mathbf{q}) + B, \quad (9)$$

where $1/M = \text{KLP}(1+\alpha)A(\mu)$ and $I(\mathbf{q}) = |yDF(\mathbf{q})/k|$. The fact that $1/k^2 = J(e^2/mc^2V)^2\lambda^3$ is independent of $\mathbf{q}$ was used here; the quantity K is a scaling factor. Evidently, the intensity of the Bragg reflection can be represented by the expression

$$I = M\left(T - \sum_m p_mI_m - B\right). \quad (10)$$

The factors influencing the accuracy of the determination of the intensities of the diffraction reflections and the moduli of the structural amplitudes can be divided into two types. The factors unrelated to the type of radiation (X-rays and neutrons) or depending on a given type but in terms details which are insignificant should be assigned to the first type. For example, as a result of repeated scattering, due to the fact that the reflecting site can contain simultaneously several inverse lattice sites, the intensity of the measured reflection changes. Such a change can be avoided when the crystal is rotated around the direction of the scattering vector until all the inverse lattice sites, except that for which the measurement is made, have passed out of the Ewald sphere. Factors of the first type also include the geometry of the measurement taken into account by the Lorentz multiplier.[6]

Factors of the second type, associated with various mechanisms of the interaction with X-rays and neutrons with the crystal, have to be taken into account in different ways (absorption, extinction, thermal diffuse scattering). The principal difficulties in the accurate determination of the structure amplitude arise in absorption when the test crystal has an arbitrary geometrical shape, in extinction in the case where the shape and size of the coherent scattering blocks in the specimen are markedly anisotropic, and in thermal diffuse scattering for crystals with a low symmetry.

The allowance for absorption when the radiation passes through the crystal reduces to the calculation of the integral[9]

$$A(\mu) = \frac{1}{v}\int_{v} \exp[-\mu(r_1 + r_2)]\, dv, \qquad (11)$$

in which r_1 and r_2 are the distances traversed by the beam in the crystal before and after diffraction. Here the accuracy of the determination of the average effective length of the path of the beam in the crystal for each *hkl* reflection is the most significant. For a spherical specimen, the corrections for absorption have been tabulated; for a polyhedral crystal, they can be calculated by a method which has been described.[7] The absorption coefficients for X-rays are in the range ~10^2–10^3 cm^{-1}, while those for neutrons are significantly smaller ($\mu \cong 10^{-1}$ cm^{-1} for $\lambda \leq 1$ Å). Lithium, boron, cadmium. and certain lanthanides ($\mu_{neutr} \cong 10$–100 cm^{-1}) as well as substances whose composition includes a large number of hydrogen atoms ($\mu_{neutr} \cong 2$–5 cm^{-1}) are exceptons.[9]

Allowance for the deviations from kinematic diffraction due to the presence of excited states in the crystal lattice in the radiation field, which entails non-elastic coherent scattering by acoustic phonons or thermal diffuse scattering (TDS) is extremely important.[8,10] Allowance for this effect is especially important in neutron diffraction, where the energy of the neutrons used in the diffraction experiment is close to that of the thermal vibrations of the lattice atoms. The contribution by TDS to individual reflections in molecular crystals can reach 30% of the intensity of the Bragg peak.

For certain relations between the velocities of the thermal neutrons and sound in the crystal, the effective cross-sections for the TDS of neutrons and X-rays can become comparable. For example, for lead and similar "soft" materials, the TDS for neutrons and X-rays become similar when $\lambda_{neutr} \leq 1.70$ Å while for "hard" materials (tungsten and others) this happens already for $\lambda_{neutr} \leq 0.77$ Å.

The correction for TDS can be represented in the form

$$1 + \alpha = \exp[2\Delta U[(\sin\theta)/\lambda]^2], \qquad (12)$$

where α is the ratio of the intensities of the thermal diffuse and Bragg scattering and ΔU is the effective temperature coefficient common to all the atoms of the structure. Evidently the neglect of the TDS effect leads to errors in the determination of the atomic thermal parameters manifested by their apparent decrease.

Several methods have been proposed for the calculation of corrections for TDS which are suitable in the case of crystals of any symmetry.[8,10] The effect can also be diminished by reducing the experimental temperature. For example, $\Delta U \cong 0.1$ Å^2 for ammonium oxalate $(NH_4)_2C_2O_4$ at room temperature, while at $T = 110$ K the quantity ΔU decreases to 0.04 Å^2. However, the use of low temperatures presupposes the thermal stability of the crystal and the absence of phase transitions in the latter. One should note that the contribution of TDS depends significantly on the conditions of the measurements: the divergence and the non-monochromatic nature of the primary beam, the aperture of the detector, the size of the crystal investigated, and the methods used to correct the background and the quantity q.[10]

As an example, Fig. 2 presents the dependence fo the TDS contribution on $(\sin\theta)/\lambda$ and the aperture of the counter for the scattering of X-rays by a ruby single crystal.[10] Such data make it possible to select the optimum strategy for precision intensity measurements.

After the above corrections have been introduced, it is possible to formulate a formal expression for the estimation of the variance of the measured intensity:

$$\sigma^2(I) = Q^2\sigma^2_{cr} + Q^2p^2I_0^2 + s^2(Q)\, I_0^2, \qquad (13)$$

where σ^2_{st} takes into account the statistical components of the variance (the radiation quanta registered by the counter obey the Poisson distribution[11]), Q is determined by comparing the intensities of periodically measured references reflections, $s^2(Q)$ is the random variance of Q, the multiplier p takes into account the instrumental instability of the error associated with the application of the corrections and partly with the random errors that have not been taken into account. An estimate of the accuracy of the measurement is also provided by averaging the symmetrically-equivalent reflections measured over the total Ewald sphere; the extent of the scattering is an index of the accuracy of the experimental determination of the extent of diffraction intensities.[12]

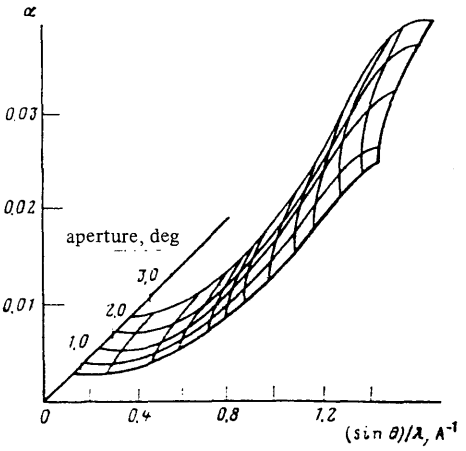


Figure 2. The influence of thermal diffuse scattering on the intensity of X-ray diffraction by a ruby single crystal.[10]

The primary treatment of diffraction data described above makes it possible to proceed to the elucidation of the structure of the crystal and then to its refinement by the method of least squares. Here it is necessary to take into account extinction and anomalous scattering. The correction for extinction allows for the change in the reflection intensity owing to the phase relations between the rays scattered by different points in the crystal. The correction is applied by introducing in Eqn. (8) the multiplier $y = y_1y_2$. The correction for the primary extinction y_1 takes this effect into account in each of the mosaic blocks and the correction for the secondary extinction y_2 takes it into account for the entire collection of these blocks. Corrections of the two types are inter-related—in particular $y_2 = f(y_1)$,[12] and only the quantity y_2 is therefore usually included among the parameters refined by the method of least squares.[13]

Anomalous scattering arises when the frequency of the incident radiation is comparable to the intrinsic frequencies of the vibrations of the scattering atom in the crystal. In this case the expression for the atomic amplitude is[7]

$$f=f_0+\Delta f'+i\Delta f'', \qquad (14)$$

where f_0 is the normal scattering component and $\Delta f'$ and $\Delta f''$ are corrections taking into account the anomalous scattering. The values of these corrections at the X-ray wavelengths normally employed in the structural analysis for light atoms are small, but for heavy atoms they can reach 5–10% of f_0. In neutron diffraction the correction for anomalous scattering is significant only for nuclei such as ^{6}Li, ^{10}B, ^{113}Cd, and certain lanthanides. The methods used to apply this correction have been described in detail and the corresponding tables of the values of $\Delta f'$ and $\Delta f''$ have been published.[14,15]

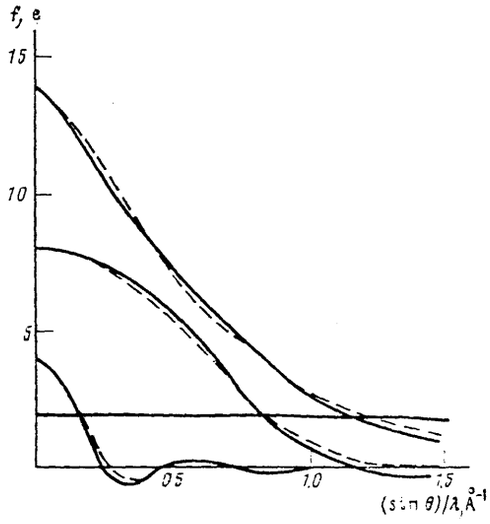


Figure 3. The atomic [$f = f_K + f_L + f_M$ (1)] and partial [f_K (2), f_L (3), and f_M (4)] scattering amplitudes for the Si atom calculated using Slater orbitals (continuous lines) and Hartree–Fock orbitals (dashed lines).[16]

We shall now consider certain features of the procedure involved in the application of the method of least squares in connection with the problem of the determination of the electron distribution in crystals. The positional (coordinates) and thermal parameters of atoms, the scaling factor k which converts the experimental data to values in terms of the absolute scale, and the correction for extinction are refined by this method. The deficiencies of the model of spherically symmetrical atoms have already been mentioned above. The error in the refinement procedure can be diminished, for example, by taking into account the fact that the electrons of the valence subshells deformed by chemical bonds scatter X-rays mainly in the "short-range" region of the inverse space. Fig.3 presents the atomic amplitude calculated using Slater type orbitals (STO) in terms of the orthogonal basis set and the basis set of the Hartree–Fock (HF) orbitals for the silicon atom[16] having the electronic configuration $1s^22s^22p^63s^23p^2$. It is also seen from Fig.3 that, when the basis set is altered, the partial amplitudes indicate an apparent "flow" of densities from one shell to another. This must be taken into account by comparing the experimental and quantum-chemical results of the determination of electron density distribution: the application of identical basis functions in both cases is an obligatory condition for the correct interpretation of the results.

The coordinates and thermal parameters of atoms are usually refined on the basis of "long range" reflections where the contribution due to spherically symmetrical (undeformed) inner electron subshells is mainly manifested.[17] Here it is assumed that the boundary between the "long-range" and "short-range" regions of the inverse space is located at $(\sin\theta)/\lambda \cong 0.7–0.8$ Å^{-1}. However, one should bear in mind that the non-spherical characteristics of the valence subshells (for example, the unshared electron pairs) make an appreciable contribution to the scattering up to $(\sin\theta)/\lambda \leqslant 1.0$ Å^{-1}.[5] Instead of refining the thermal and positional parameters of atoms, we can also determine them in an independent neutron diffraction experiment.

In accurate studies the modification of the electron density of atoms in the crystal is taken into account approximately by introducing into the radial part of the function describing the density of valence electrons the multiplier κ which characterises its "contraction" or "expansion" compared to the free atom.[18] In this case the scattering amplitude for valence electrons is defined by the expression

$$f_{val}(\varkappa, q)=f'(q/\varkappa), \qquad (15)$$

where f' is the amplitude of the scattering by the free atom.

The parameter κ and the populations of the valence shells of atoms are included among the parameters refined by the method of least squares. An even greater flexibility can be achieved by employing a multipolar model. Within the framework of this model, the electron density of the bound atom in the crystal is represented by the expansion in terms of the angular harmonics $y_l(\theta, \phi)$ satisfying the local symmetry of the environment (see below). This model diminishes significantly the R factor#[13] and other criteria for the statistical estimation of the reliability of the results.[19]

Allowance for a series of physical and chemical requirements, such as the electroneutrality of the crystal, the equality of the parameters referring to chemically equivalent parts of the molecules, and the imposition of limitations on the components of the thermal vibrations owing to the rigidity of the bond,[20] is also extremely useful and makes it possible to reduce the error of the results.

III. METHODS FOR THE REPRESENTATION OF ELECTRON DENSITY

In the study of the characteristics of the electron distribution in a system made up of atoms linked by chemical interactions, it is convenient to make use of difference functions of the type

$$\delta\rho(\mathbf{r})=\rho_1(\mathbf{r})-\rho_2(\mathbf{r}), \qquad (16)$$

where ρ_1 and ρ_2 are functions corresponding to two different

---

#The unreliability factor R is used to estimate the relative error in the refinement of the structure of the crystal and is calculated from the formula $R = \sum_{\mathbf{q}}[F_{exp}(\mathbf{q}) - F_{calc}(\mathbf{q})]/\Sigma F_{exp}(\mathbf{q})$, where F_{exp} and F_{calc} are the measured and calculated structural amplitudes respectively.

versions of the determination of the electron distribution. The experimental electron density ρ_{exp} is normally employed as ρ_1.

The function of the deformation electron density

$$\delta\rho(\mathbf{r}) = \rho_{exp}(\mathbf{r}) - \sum_n \rho_n(\mathbf{r}), \qquad (17)$$

is most convenient for the analysis of the redistribution of electrons in the system caused by the involvement of atoms in chemical bonding. Here the sum represents the electron density for a set of spherically symmetrical atoms located at the same point as the atoms in the crystal (the electron density of the "promolecule").[21]

If only the inner electrons (electronic skeletons) of atoms are involved in the summation, then the function $\delta\rho$ describes the valence electron density of the crystal.

Eqn.(17) can be rewritten in terms of the series

$$\delta\rho(\mathbf{r}) = \frac{1}{V}\sum_{\mathbf{q}} \delta F(\mathbf{q}) \exp(-i\mathbf{qr}), \qquad (18)$$

where $\delta F(\mathbf{q}) = F_{exp}(\mathbf{q}) - F_{calc}(\mathbf{q})$ and $F_{calc}(\mathbf{q})$ is the Fourier transform of the electon density of the promolecule.

The theoretical calculation should be performed using modern quantum-chemical methods[3] taking into account the relativistic effect and multiconfiguration interaction; otherwise the low accuracy of the calculation can hinder the interpretation of $\delta\rho$. However, since this is not always feasible, one can employ wave functions calculated with the aid of the relativistic version of the Hartree–Fock method; the corresponding f curves have been tabulated.[7]

The function $\delta\rho$ can be regarded as one describing the redistribution of electrons in the system due to chemical bonding. Naturally the diffraction data must be interpreted in terms of the same basis set as in the calculation for the promolecule taking into account the modification of the wave functions of the valence electrons.

The graphical representation of the cross-sections of the deformation electron density function for the test molecules makes it possible to determine whether the chemical bonds are straight or bent (strained) and directional or of the many-centre type, what their shape is in cross-section, where the unshared electron pair density maxima are located, how the deformation of the electron density of the atom depends on its environment, etc.

As an example, Fig.4 presents the results of a precision study of a ruby crystal having the composition Al_2O_3 + Cr(0.46 wt.%).[22] Fig.4*a* illustrates the map of the deformation electron density of a fragment of the structure of ruby containing characteristic Al–O bonds 1.970 and 1.856 Å long. The map contains excess deformation (covalent) peaks whose height is approximately 0.27 eÅ^{-3} which have undergone a shift towards the more electronegative O atom and which have been displaced from the line of the bond. This map shows that the Al–O bonds in ruby and also in corundum Al_2O_3 are partly covalent and strained and the shift of the deformation peak from the line of the bond is a consequence of the electrostatic interaction of the electrons in the region of the bond with the nearest "foreign" positively charged ion. It can be seen that distinctly directional individual chemical bonds characteristic of ionic crystals are absent from the structure, while the electron density is highly localised. These features of the electronic structure are reflected in the properties of ruby such as, for example, its mechanical strength.

In the study of ruby[22] an attempt was made to determine by X-ray diffraction the positions of the Cr^{3+} ions. Refinement by the least squares method (R = 0.0068) showed that the chromium ion, substituting the Al^{3+} ion in the structure isomorphously, is not located exactly at the position of the latter but is displaced along the hexagonal z axis by 0.13 Å towards an octahedral vacancy. A difference electron density map has been constructed (Fig.4*b*) on which the admixture of Cr^{3+} ions appears in the form of an excess peak 0.3 eÅ^{-3} high in the vicinity of the Al^{3+} ions. The possibility of determining such a small amount of the admixture is characteristic of the actual attainable accuracy of modern diffraction methods.

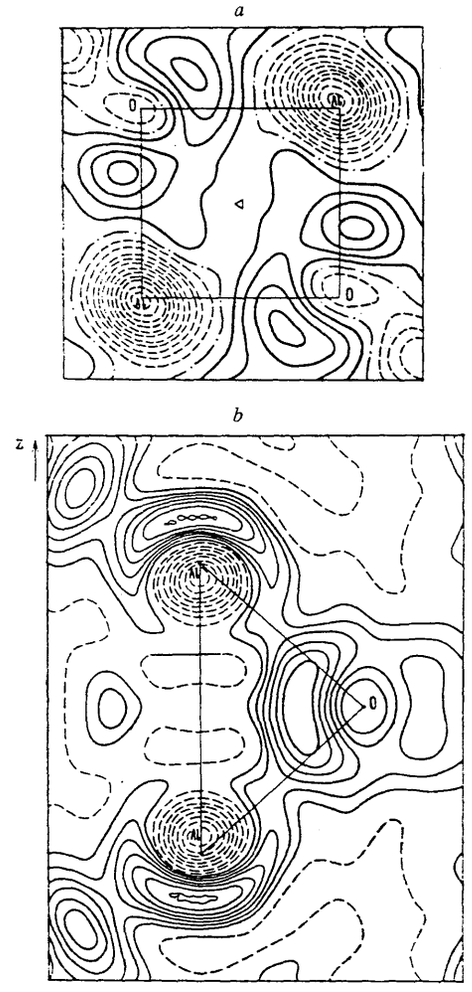


Figure 4. Fragments of deformation electron density in the ruby crystal.[22] (Here and henceforth the continuous lines on the map connect points with excess electron density, the dashed lines connect points with deficient electron density, and the dash-dot lines connect points with zero electron density): *a*) sections through the Al and O atoms and the centre of symmetry; the spacing between lines 0.07 eÅ^{-3}; *b*) the (0110) [sic] plane; the Cr atom was not removed in the synthesis and can be seen as a peak above and below Al; the spacing between lines is 0.05 eÅ^{-3}.

The deformation electron density function can be constructed in accordance with two schemes.[23,24] In the first of these all the parameters for the calculation of F_{calc} were

obtained by refining the X-ray diffraction data corresponding to high experimental values of $(\sin\theta)/\lambda$ (the $X-X$ method). In the second F_{calc} is determined with the aid of parameters obtained from a neutron diffraction experiment (the $X-N$ method). As stated above, the advantage of the latter consists in the absence of a dependence of the results of the measurements of the model of the electronic structure of the crystal and in the reliability of the determination of the positional and thermal parameters of light atoms (in the first place hydrogen) in the presence of heavy atoms.

The application of the $X-N$ approach requires allowance for the specific features of both diffraction methods and also for the possible difference between the temperatures of the two experiments.[12,23] A check on the temperature can be carried out by calculating the unit cell parameters of the crystal, which should be identical at identical temperatures. It is more difficult to take into account other effects. For example, TDS is manifested in different ways in experiments of the two types: in neutron scattering the contribution of TDS is greater. This reduces the thermal parameters of the atoms obtained in neutron diffraction experiments by approximately 10% relative to the X-ray experiments. Next, discrepancies arise in the results due to the differences in the allowance for the background in the calculation of the contribution of elastic scattering to the intensity. Furthermore, the different sizes of the crystals and the difficulty of an adequate description of the X-ray and neutron scattering processes also lead to errors which cannot be always fully corrected. Practical procedures used in such corrections can be found in a number of communications.[1,12,23]

In order to obtain reliable results in the analysis of the function $\delta\rho$, the error in the deformation density $\sigma(\delta\rho)$ must be less than the significant details in the function $\delta\rho$. On the basis of the standard deviations of the parameters obtained as a result of the least squares refinement and $\sigma^2(F_{exp})$, the variance of the deformation electron density can be represented in the form[23,25]

$$\sigma^2(\delta\rho) = \frac{2}{V^2}\sum_{|q|>0}[\sigma^2(\delta F)\cdot\cos^2\alpha + \delta F^2\cdot\sin\alpha\cdot\sigma^2(\alpha) + \\ + \sin 2\alpha\cdot\delta F\cdot\sigma(\delta F)\cdot\sigma(\alpha)\cdot\gamma(\delta F,\alpha)], \qquad (19)$$

where $\alpha = \mathbf{qr} - \beta$, β is the δF phase, and γ the correlation coefficient.

As a result of a careful study, it is possible to express $\sigma^2(\delta\rho)$ in terms of $\sigma^2(F)$, $\sigma^2(F_{calc})$, and $\sigma^2(k)$ and to show that (1) the error due to $\sigma^2(F)$ and $\sigma^2(F_{calc})$ is approximately constant throughout the cell and does not exceed 0.04 eÅ^{-3} for centrosymmetrical structures with light ($Z \leq 16$) atoms and 0.06 eÅ^{-3} for non-centrosymmetrical structures and (2) the error due to $\sigma^2(k)$ and the errors in the structural parameters is significant only in the vicinity of the centres of atoms and for heavy ($Z \geq 50$) atoms reaches in this instance 6–8 eÅ^{-3}, while for light atoms it is 0.1–0.8 eÅ^{-3}. In the $X-N$ scheme the error associated with the inaccurate selection of the amplitude of the coherent neutron scattering can also have an effect; in the vicinity of the centres of atoms it is comparable in magnitude to the errors due to other factors and must be taken into account.[26]

The average error of the determination of the deformation electron density, constructed on the basis of precision diffraction data, is usually less than 0.05 eÅ^{-3} in the region of the chemical bond.[1] This makes it possible to investigate at the present time the details of the electron distribution in crystals containing heavy atoms (up to $Z = 78$). Such accuracy and the potential set of objects, including complex molecules with heavy atoms, are so far inaccessible to theoretical calculations.

Another field where diffraction data are used involves the determination of the numerical characteristics of the electron distribution. Several methods have been proposed for the solution of this problem and these have been described in detail, for example, by Tsirel'son and Ozerov.[23] The simplest method of parametrising the function $\rho(\mathbf{r})$ consists in determining the electronic charge concentrated in a certain volume by the direct integration of the function ρ over this volume. In particular, it is possible to estimate in this way the effective atomic charges. Usually the volume over which the integration is carried out is represented by a sphere bounded by the minimum of the function ρ; this approximation is justified only for a simple ionic compound.[24] In the case of atoms involved in covalent bonds, it is useful to employ more complex methods for charge separation. In the integration, account must also be taken of the fact that the function ρ is constructed on the basis of data obtained in a diffraction experiment in which only a limited number of terms of the Fourier series are measured; the appropriate correction must therefore be applied to the final results.[27]

Table 1. The atomic charges in certain silicates.[28]

Atom	$Mg_2Si_2O_6$	$Co_2Si_2O_6$	$Fe_2Si_2O_6$	Mg_2SiO_4	Co_2SiO_4	Fe_2SiO_4
Metal, $M(1)$	+1.84 (4)	+1.29 (11)	+1.14 (12)	+1.76 (3)	+1.60 (11)	+0985 (8)
Metal, $M(2)$	+1.79 (4)	+0.81 (12)	+1.10 (13)	+1.74 (3)	+1.54 (7)	+1.45 (11)
Si^A	+2.20 (4)	+1.79 (9)	+2.21 (11)	+2.11 (3)	+2.21 (10)	+2.43 (6)
Si^B	+2.36 (4)	+2.76 (9)	+2.16 (11)	—	—	—
$O(1)^A$	−1.51	−1.10	−1.04	−1.52	−1.24	−1.13
$O(1)^B$	−1.37	−1.14	−1.19	—	—	—
$O(2)^A$	−1.36	−1.12	−1.09	−1.29	−1.24	−1.21
$O(2)^B$	−1.43	−1.16	−1.20	—	—	—
$O(3)^A$	−1.31	−0.84	−0.92	−1.40	−1.39	−1.24
$O(3)^B$	−1.22	−1.10	−1.18	—	—	—
⟨Metal⟩	+1.82	+0.95	+1.12	+1.75	+1.57	+1.15
⟨Si⟩	+2.28	+2.28	+2.19	—	—	—
⟨O*⟩	−1.42	−1.43	−1.13	—	—	—
⟨O**⟩	−1.27	−1.05	−0.97	—	—	—
⟨O⟩	−1.37	−1.08	−1.10	−1.40	−1.29	−1.19

Notation: The angular brackets indicate that average quantities are quoted; $M(1)$ and $M(2)$ are two types of octahedral and A and B are two types of tetrahedral positions in the structure.

*Non-bridging oxygen atoms.

**Bridging oxygen atoms.

The effective charges on the atoms in certain oxides and silicates obtained in this way[27,28] are listed in Table 1. In conformity with modern ideas concerning the semicovalent character of the chemical bond, the charges on the oxygen ion in the oxide compounds are in the range from −0.8 to −1.5 e and those on the silicon atoms are from +1.8 to +2.8 e.

Another way of estimating the atomic charges from diffraction data consists in the application of the method of least squares.[29] For this purpose, the atomic electron shells are assumed to consist of a constant inner part to which a fixed number of electrons are bound and of the valence part whose electron population is to be refined. Simultaneously with the refinement of the number of valence electrons, it is possible to take into account, using the parameter κ and Eqn.(15), the radial modification of the valence electron shell associated with the charge redistribution in the system.[18]

A correlation has been observed between the charge on the atom and the parameter κ,[18] which agrees well with the familiar Slater rules for the selection of the exponential multipliers in the radial parts of the orbitals. Fig.5 shows that these simple rules make it possible to determine quite satisfactorily the charge on the N atom in various organic compounds; this can also be said of the C and O atoms.

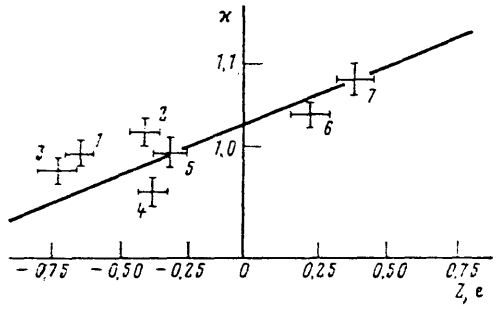


Figure 5. Dependence of κ on the atomic charge according to Coppens et al.:[18] 1) and 2) glycylclycine; 3) formamide; 4) cyanuric acid; 5) tetrasulphotetranitride; 6) sulphamic acid; 7) *p*-nitropyridine *N*-oxide; the result of the calculation by the Slater method is indicated by the straight line.

We shall consider the multipolar procedure for the refinement of structural parameters by the least squares method. In this approach the electron density of the crystal is represented in the form

$$\rho(\mathbf{r}) = \sum_j \left\{ \rho_j(\mathbf{r}) + \sum_i c_{ij} R_{ij}(\mathbf{r}) \Phi_{ij}(\theta, \varphi) \right\} \qquad (20)$$

where ρ_j is the electron density on the jth atom, according to Hirshfeld and Harel,[30,31] or on the skeleton of this atom, according to Stewart,[32] and the c_{ij} are the coefficients of the expansion (the electron "populations") of the multipoles.

Eqn.(20) represents the expansion of the deformation of the valence electron density in terms of functions whose angular component Φ_{ij} describes the multipolar (dipolar, quadrupolar, octapolar, etc.) deformation of the atom in the crystal, determined by the symmetry of the environment and the effects of the chemical interaction. The radial functions usually have the form

$$R_{ij}(r) \sim r_{ij}^n \exp(-2\alpha_{ij} r_{ij}),$$

where r_{ij} is the current coordinate reckoned from the nucleus of the jth atom.

Thus the electron density of the crystal is represented by the sum of the multipolar terms ("pseudoatoms"[32]) and the coefficients and the experimental multipliers of the multipoles α_{ij} are included among the parameters refined by the least squares method. This model is very flexible, and its flexibility can be increased still further by combining the multipolar expansion method with the use of the parameter κ.[19] The electron populations of the monopolar terms are usually interpreted as the electronic charges on the atom. A direct interpretation of the remaining multipolar parameters of the electron density distribution in terms of the LCAO-MO approximation is difficult.

The multipoles linked by the *d* orbitals of transition metal atoms are an exception.[33] Information of this kind is of considerable interest. Thus it follows from the refinement of the above populations of the cobalt atom in (*meso*-tetraphenylporphyrinato)cobalt(II) ($C_{44}H_{28}N_4Co$),[34] carried within the framework of the crystal field theory, that the cobalt atom in this compound exists in a low-spin state, in conformity with the results of magnetic measurements (Table 2).

Table 2. The electron populations of the *d* levels of cobalt in $C_{44}H_{28}N_4Co$.[34]

Atomic orbital	Electron populations			
	I	II	III	III
$b_1 (d_{x^2-y^2})$	1.4	0.0	1.0 (2)	0.25
$a_1 (d_{z^2})$	1.4	1.0	1.0 (2)	1.06
$b_2 (d_{xy})$	1.4	2.0	1.3 (2)	1.76
$c (d_{xz}, d_{yz})$	2.8	4.0	3.7 (3)	3.91

Notation: I) the expected high-spin state; II) the ideal low-spin state; III) results of refinement on the basis of diffraction data; IV) theoretical calculation by the configuration interaction method.

The observed deviation from the expected values indicates the limited applicability of the one-determinant approximation for the description of the observed picture. Comparison with theoretical calculations (Table 2) show that, when the additional excitations of the electronic configurations are taken into account, the theoretical populations of the 3*d* orbitals vary in parallel with experimental data. Another important result of Stevens' study[34] is the demonstration of the limited character of the crystal field theory, which is frequently used to interpret the state of the metal ion in organometallic [sic] compounds.

In particular, the unduly high populations of the $d_{x^2-y^2}$ orbital which follow from the diffraction data are a consequence of the failure to take into account the metal–ligand σ-bond by this theory, while the neglect of the π interaction leads to reduced populations of the d_{xy} and d_{yz} orbitals.

The large number of parameters of the multipolar model entails their strong mutual correlation in the equations of the least squares method. In order to increase the reliability of the results of the multipolar method of calculation, it is useful to introduce certain additional conditions relating the parameters being refined to one another. For example, it is possible to carry out the refinement in such a way that agreement is ensured between the electric field gradient at one of the atomic nuclei and the value derived from NQR experiments. A refinement of this kind, carried out for aluminium phosphate ($AlPO_4$)[35] showed that the above procedure makes it possible to attain a deeper minimum in the functional (3) for the charges on the Al, P, and O atoms; values of +1.4, +1.0, and −0.60 e respectively were obtained. These charges indicate a significant covalence of the P–O bond, which has also been confirmed by the cross-sections of the deformation electron density function constructed by Schwarzenbach and Ngo Thong.[35]

The multipolar analysis of the distribution of electron density in diamond and graphite has shown that the exponential multiplier in the radial function α_{exp}, found by least

squares refinement, is 1.56 for diamond[36] and 1.58 for graphite,[37] whereas for the free carbon atom $\alpha = 1.59$.[38] Comparison of these data with the molecular optimised value $\alpha_m = 1.72$, obtained for the carbon atom by averaging the results of quantum-chemical calculations in terms of the minimal basis set for a series of simple organic molecules,[38] has shown that the calculated α corresponds to a more "contracted" atom. An analogous situation has been observed for silicon ($\alpha_{exp} = 1.6$; $\alpha_m = 1.75$).[38] Comparisons of this kind are useful for semiempirical quantum-chemical calculations where there is a possibility of choosing the optimum values of the exponential multipliers, defining the basis functions, depending on the level of the approximations adopted. Thus one may conclude that in quantum-chemical calculations where the overlap of orbitals of neighbouring atoms is neglected it is possible to compensate for the failure to allow for the shift of part of the electron density to the interatomic space by reducing the values of α in terms of the minimal basis set.

Maps of the deformation electron density can be constructed on the basis of the results of the multipolar refinement. Such "synthesised" maps filter out the "noise" associated with the errors in the diffraction data and are to a large extent free from the defects due to the cut-off of the Fourier series.[19] As an example, we shall consider the compound $C_{44}H_{28}N_4Co$ mentioned above.[34] Fig. 6*a* presents the cross-section of the multipolar function $\delta\rho$ in the plane of the pyrrole ring averaged with respect to the chemically equivalent parts of the molecule. The distribution of errors for the non-averaged case is illustrated in Fig. 6*b*; the error in the determination of the distribution of the centres of atoms reaches 0.7 eÅ^{-3} according to the estimates made above. The "multipolar filtration" and averaging reduce this error by a factor of 3–4. Ultimately the characteristics $\delta\rho$ become even more pronounced: $\delta\rho > 3\sigma(\delta\rho)$. The peak on the C(2)–C(3) bond on the map, which significantly exceeds the peaks on other covalent bonds in the porphyrin molecule, is striking. This finding has been analysed[34] and accounted for in terms of the localisation of the π electrons at this bond.

Another quantitative approach to the analysis of the electron distribution in crystals is based on the representation of $\rho(\mathbf{r})$ with the aid of the linear combination of atomic orbitals (LCAO) in the following form:

$$\rho(\mathbf{r}) = 2\sum_{ij} P_{ij}\varphi_i(\mathbf{r})\varphi_j^*(\mathbf{r}) \qquad (21)$$

where ϕ_i are the analytical atomic orbitals (for example, the orthogonalised Slater orbitals) and P_{ij} are the elements of the charge–bond order matrix characterising the electronic structure of the system investigated. Having calculated the Fourier transform of formula (21), it is possible to find the matrix elements P_{ij} assuming them to be adjustable parameters and minimising the functional (3). However, the attempt to apply such an approach in conjunction with the least squares matrix encountered computational difficulties associated with the correlation between the parameters to be refined.[39–44] This led to the use of the palliative methods mentioned above,[29] in which either certain matrix elements P_{ij} were not refined, being selected *a priori*, or the electron populations of the valence shells of each atom were refined as one parameter. Nevertheless, the idea of the above approach is extremely primising because it leads to the possibility of a direct comparison of the experimental results with data obtained from quantum-chemical calculations in terms of the LCAO approximation involving the same matrix P.

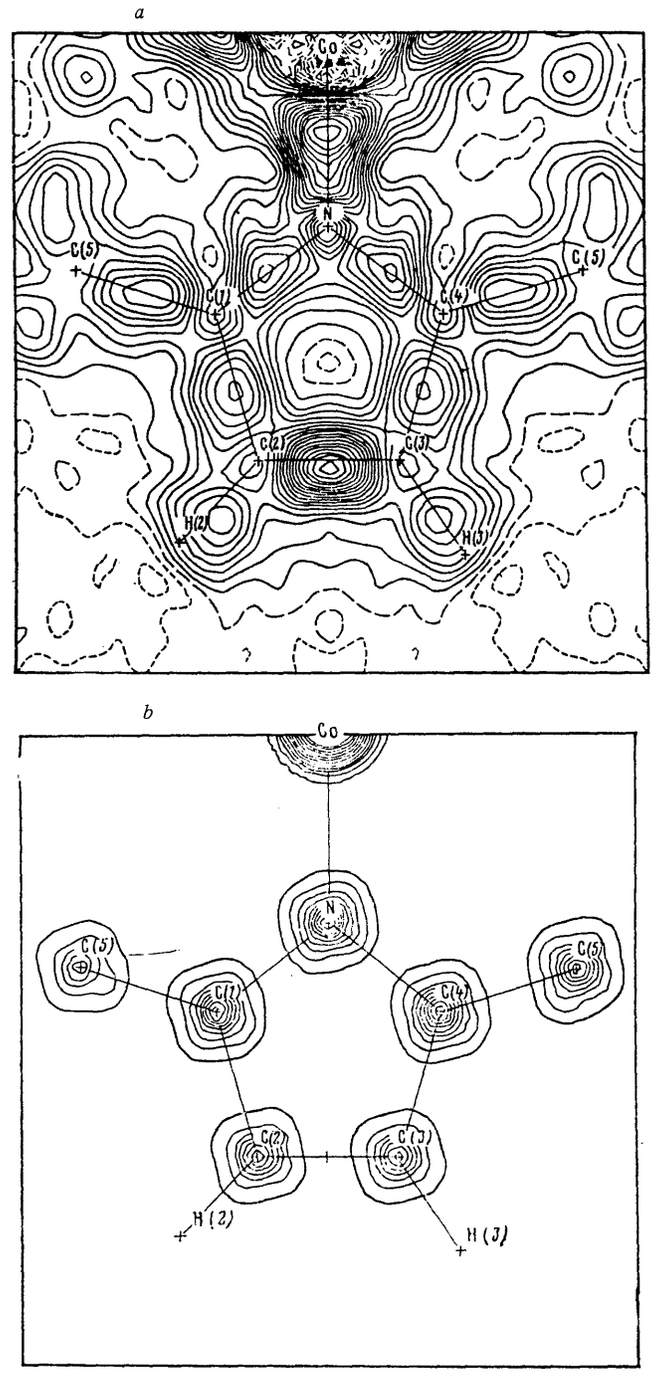


Figure 6. Deformation electron density for the $C_{44}H_{28}N_4Co$ crystal according to Stevens:[34] *a*) section in the plane of the pyrrole ring (spacing between lines 0.05 eÅ^{-3}); *b*) distribution of errors on the deformation electron density map (spacing between lines 0.02 eÅ^{-3}).

Analysis[45–47] has shown that, when the matrix elements P_{ij} are sought, account must be taken of the quantum character of the electron distribution. In particular, it is essential that the quantities found should describe the distribution of electron density consistent with the Pauli

principle. Neglect of this fact can lead to negative electron densities in the vicinity of the nucleus or to populations of molecular orbitals exceeding 2e.[48] Allowance for it[47] led to equations for P_{ij} having the same form as the equations for the same matrix in quantum chemistry (the Hartree–Fock–Roothaan equations). Thus the rigorous analysis made it possible to reduce to a single formal basis the experimental and theoretical approaches to the study of the distribution of electron density.

Table 3. The effective atomic charges in $HCOOLi.D_2O$.[49]

Atom	Atomic charges, e		
	experiment	*ab initio* calculation	EHM calculation
	Lithium ion		
Li	0.82	0.70	0.55
	Formate ion		
C	0.04	−0.01	−0.01
O (1)	−0.53	−0.34	−0.30
O (2)	−0.46	−0.34	−0.26
H	0.13	−0.02	−0.02
	Water molecule		
D (1)	0.11	0.06	0.08
D (2)	0.07	0.06	0.07
O (3)	−0.18	−0.12	−0.10

Table 4. The intermolecular interaction energy U_M and the heat of sublimation ΔH_S for the $HCOOLi.D_2O$ crystal.[50]

Method of calculation	U_C, kcal mol^{-1}	U_M, kcal mol^{-1}	ΔH_S, kcal mol^{-1}
Diffraction data	34.78	50.02	49.05±0.05
Extended Hückel method	8.36	24.10	—
Ab initio calculation	8.48	23.72	—

Remarks: U_C is the Coulombic interaction energy; ΔH_S was measured on a Calvet microcalorimeter.

Calculations for the lithium formate deuterate ($HCOOLi.D_2O$) crystal[49] have shown (Table 3) that, although the experimental results agree with quantum-chemical data, there are also differences reflecting the effect of the crystal environment (both types of calculations have been carried out in terms of the same basis set). This has been manifested distinctly in the calculation of the intermolecular interaction energy in the $HCOOLi.D_2O$ crystal.[50] Calculation of this quantity by the method of atom–atom potentials taking into account the Coulombic interaction in terms of the "experimental" and quantum-chemical (for individual molecules) charges in the atoms revealed a satisfactory agreement with the results of thermodynamic measurements only when the "experimental" charges were used (Table 4). On this basis, one may conclude that the P_{ij} matrix obtained from diffraction data describes satisfactorily the distribution of electron density in the crystal investigated. Theoretical calculations taking into account the crystal environment are not so effective.

IV. THE ELECTROSTATIC FIELD IN THE CRYSTAL

The methods involving the "point" and parameteric representations of the electron density function using diffraction data were examined above. A concept according to which diffraction data are used to determine the electrostatic potential in crystal has developed recently.

The analytical expression relating the charge density functions for the electrons and nuclei of a system to the electrostatic potential of the point **r** is defined by the Poisson equation and assumes the following form:

$$\varphi(\mathbf{r}) = \sum_i (Z_i/|\mathbf{R}_i - \mathbf{r}|) - \int_{-\infty}^{\infty} \frac{\rho(\mathbf{r}')}{|\mathbf{r}' - \mathbf{r}|}\, d\mathbf{r}, \qquad (22)$$

where Z_i is the charge on the atomic nucleus located at the point $\mathbf{R}_i$. The first term in Eqn.(22) describes the contribution to $\phi(\mathbf{r})$ by the nuclei in the system and the second describes the contribution by the electron distribution. The function $\phi(\mathbf{r})$ characterises the electrostatic interactions between the unperturbed system and the positive unit charge at the point **r**. Eivdently the potential $\phi(\mathbf{r})$ can be useful in the description of the chemical interaction when the molecules are separated by large distances, whereupon one can neglect the polarisation, charge transfer, and exchange effects.

Numerous chemical applications of this approach have been dealt with in detail in a communication.[51] However, the deformation electrostatic potential (DESP), introduced by Varnek et al.[52] and Spackmann and Stewart,[53] contains no less information and is defined by the expression

$$\delta\varphi(\mathbf{r}) = \int_{-\infty}^{\infty} \frac{\delta\rho(\mathbf{r}')}{|\mathbf{r} - \mathbf{r}'|}\, d\mathbf{r}' = -\frac{4\pi}{V} \sum_{\mathbf{q}} \frac{\delta F(\mathbf{q})}{|\mathbf{q}^2|} \exp(-i\mathbf{q}\mathbf{r}). \qquad (23)$$

From the physical point of view, DESP characterises the electrostatic field, which, when superimposed on the electrostatic field of the promolecule, ensures a stable equilibrium configuration of the system.

Fig.7, obtained for ruby, shows that DESP reflects its physical properties.[22] In particular, the delocalisation of electron density discussed above leads to an unusual distribution of the electrostatic potential in the ruby crystal. The regions near the centres of the aluminium atoms, where the positive potential of the incompletely shielded nuclei predominates in the crystal, giving rise to quasi-continuous bands between which are included regions of negative potential extended along the Al...Al bond. Such distribution of DESP reproduces the characteristics of the electrostatic interaction of the ions in the ruby crystal and can be associated with its mechanical strength.

The electrostatic potential determines the electric field and its gradient at any point within the crystal. The knowledge of the latter is particularly important at the sites where the nuclei of the system are located, because this makes it possible, in principle, to calculate the nuclear quadrupole moment from the diffraction data without resorting to its measurement by the NQR method of with the aid of the Mössbauer effect.[54] Comparison of such results, obtained with the aid of various methods, can serve as a significant criterion of the quality of the determination of the electron distribution. The joint application of both methods in the multipolar refinement was discussed above for $AlPO_4$.[35]

The most promising applications of the experimental electrostatic potential were apparently associated with the development of the concept of a density functional based on the Hohenberg–Kohn theorem[55] and its generalisation.[56,57] According to this theorem, the energy and other characteristics of the many electron system are fully determined by

the function ρ. The exact form of this functional has not been established, but there exist many approximate relations which enable one to express the energy of the system as a functional of $\rho(\mathbf{r})$[58] or $\phi(\mathbf{r})$.[59] The first attempt to include diffraction data within the framework of such an approach[52,60] indicates that this procedure is promising for the study of the properties of crystals.

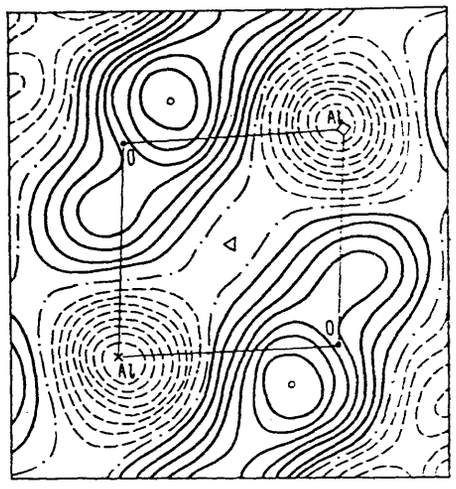


Figure 7. Experimental electrostatic deformation potential in ruby.[22]

V. THE ATOMIC (ONE-PARTICLE) POTENTIALS

The deration of the elementary step of the interaction of radiation with matter is approximately 10^{-18} s and the characteristic time of thermal vibrations of lattice atoms is 10^{-12}–10^{-13} s. However, in real measurements the diffraction experiment yields a time-average picture of the crystal structure. As mentioned above, thermal movement is taken into account by introducing individual atomic temperature multipliers $W(\mathbf{q})$, which are the Fourier transforms of the distribution function $t(\mathbf{R})$ for the positions of the nuclei (neutrons) or the centres of gravity of the electron shells of the atom (X-rays). In the high-temperature limit (classical approximation), the above function can be written in the following form having replaced the time average by the average with res0ect to the ensemble:

$$t(\mathbf{R}) = \frac{\exp(-V(\mathbf{R})/kT)}{\int_{-\infty}^{\infty} \exp(-V(\mathbf{R})/kT)\,d\mathbf{R}}, \qquad (24)$$

where $V(\mathbf{R})$ is the potential energy of the atom vibrating in the effective force field of its neighbours. Such a one-particle model[61] constitutes a development of Einstein's model of independent oscillators.[62] If $V(\mathbf{R})$ is expanded in a power series in terms of displacements reckoned from the equilibrium position and the quasi-harmonic approximation is used,[61] then the expansion coefficients characterise the effective potential of the given atom. They can be included among the parameters capable of being refined by the least squares method and hence one can obtain important information about the dynamics of the crystal lattice. We may note that the above expansion is not restircted to the harmonic terms of the series and can be extended to higher-order terms associated with the asymmetry of the potential well.

There exists a fundamental relation between the function $\rho(\mathbf{r})$ and the effective atomic potentials, established by the Gel'man–Feynman theorem.[63,64] According to the latter, the force acting on each nucleus in the system is determined by the distribution of electron density and other nuclei. For the equilibrium configuration, this force becomes zero, which can serve as a criterion of the accuracy of the experimental distribution of electron density.

Diffraction analysis of the detailed characteristics of the lattice dynamics has become possible only very recently. Its first applications were associated with the study of the ionic conduction in solids.[65–68] For example, the form of the effective potential in lithium nitride (Li_3N) has been established[67,68] from X-ray diffraction data obtained over a range of temperatures. The above compound crystallises in the *P6/mmm* group, the N atom being surrounded by eight Li atoms in the form of a hexagonal bipyramid. Having applied the 6th-order Gram–Charlier expansion§, Schulz and Zucker[66,67] showed that the height of the potential barrier between the lithium atoms located in a plane perpendicular to the c axis is 0.29 ± 0.04 eV. Thus, the appearance of ionic conduction requires that the activation energy for the ion should be in the range 0.25–0.33 eV, which agrees with the results of the experimental measurement of this quantity (approximately 0.29 eV).[68]

Another application of the approach considered has been described in a study[69] where the concept of the effective atomic potential was applied in a correct interpretation of the deformation electron density maps for the $KCuF_3$ crystal subjected to Jahn–Teller distortion. In particular, it has been shown that the Coulombic attractive interaction between the Cu^{2+} and F^- ions exerts a greater influence on the anharmonicity of the vibrations of the Cu^{2+} ion than the repulsion between the atomic skeletons.

The concept of effective atomic potentials has proved to be extremely useful also in other fields of study of the properties of crystals. Thus the parameters of the potentials can be related to the force constants of the chemical bonds and their characteristic frequencies, which makes it possible to relate the diffraction and spectroscopic analytical methods. Furthermore, knowledge of potential function character in the vicinity of atomic centres combined with knowledge of the details of the electron distribution in crystals is essential for understanding the mechanism of chemical reactions in the solid phase and also for controlling these reactions.[70] The establishment of relations of this kind is a task for the future and the immediate development of this field holds out very much promise.

VI. CHARACTERISTICS OF THE ELECTRONIC STRUCTURE OF CRYSTALS OF DIFFERENT TYPES

The possibilities of modern diffraction methods for the study of the electronic structure and properties of crystals were demonstrated above. It is important, in principle, that ρ is the observed experimental quantity which can be visualised by a graphical representation. This function contains important information about the properties of matter and with its aid it is possible to formulate a number of tasks

§ Other versions of the expansion of the potential are also possible—see, for example, Zucker and Schulz.[65]

involving the properties of the ground states of molecules and crystals.[71] The first attempts to apply this approach to the determination of certain magnetic and optical properties of crystals have already demonstrated its effectiveness.[71]

Analysis of the electron density function makes it possible to reinterpret the classical concepts of crystal chemistry. This applies particularly to the problem of the "dimensions" of atoms in the crystal and the possibility of an experimental estimation of their "radii" and "charges". In crystals with maximum covalent and metallic character, the atomic radius is determined simply as half the shortest interatomic distance and the effective charge within the limits of a sphere defined by such a radius can be logically assumed equal to zero.

However, analysis of the electron density distribution even in such simple crystals indicates a deviation of the form of the atoms in the crystal from the spherical shape. For covalent crystals of the type of diamond, the existence of electron density "bridges" between the atoms, surrounding one another in a tetrahedral arrangement has long been established. This picture corresponds to the model involving the sp^3 hybridisation of the valence orbitals of carbon and its analogues proposed by Pauling as early as 1929. It has recently been found that a situation similar to that already described is observed in metals and that a fraction of the valence electrons are localised along the length of the M–M bond.[72] The problem of the determination of the size of atoms in complex chemical compounds gives rise to even greater difficulties even when data concerning the distribution of electron density are available.

In order to obtain the dimensions of the ions from the function ρ, the criterion of the electron density minimum, characterised by the optimum separation radius R_{sep}, has been put forward.[27] It was found that the experimental values of R_{sep}, determined along the line of the bond, are intermediate between the classical and ionic and covalent (atomic) radii even in the most ionic compounds such as halides and oxides.[24] There are two main reasons which can account for this phenomenon:[73] (1) the anisotropic expansion of the electron shell of the cation and the contraction of the electron shell of the anion in the crystal and (2) the incompletely ionic character of the chemical bond. The first factor, which was initially predicted theoretically, was subsequently repeatedly confirmed also experimentally and with the aid of accurate calculations for alkali metal halides, where the bond can be regarded as virtually purely ionic. For these compounds, the experimental radii of the cations are greater by approximately 0.2 Å and those of the anions are smaller by the same amount from the classical ionic radii. This systematic difference is confirmed by the data presented in Table 5. It can be attributed wholly to the effects of the "contraction–expansion" of the ion in the crystal field and of the transfer of charge ensuring the fulfilment of the Pauli principle.

For multicharged ions in halides, oxides, and chalcogenides, these effects cannot be regarded as the only cause of the difference between the experimental maximum separation radii and the classical ionic radii. This is also indicated by the experimental estimates of the effective atomic charges obtained from the distribution of electron density, which were described above. In conformity with data obtained by other methods, these results indicate a semicovalent character of the chemical bond in the oxide and silicates of bivalent and tervalent elements. Experiment has shown that the Si–O bonds in silicates are more than half-covalent. On the other hand, chalcogenides are more correctly regarded as covalent compounds with a proportion of ionic character. This means that the concept of ionic radii cannot be strictly speaking applied at all to compounds of this group. Indeed, the results of numerous studies have shown that the optimum separation radii for the oxides and silicates are intermediate between the ionic and atomic radii and in many instances (Si, Al, Co, and Ni) they are closer to atomic radii than to ionic radii.

Table 5. Comparison of the radii of optimum separation of the electron densities of ions with the classical ionic radii (R_i) and atomic radii (R_{at}) in certain halides.

Element	R_i, Å	R_{sep}, Å	R_{at}, Å	Refs.
Na^+	1.02	1.21±0.05	1.80	[74]
Cl^-	1.81	1.61±0.05	1.00	
K^+	1.38	1.45±0.07	2.20	[74]
Cl^-	1.81	1.70±0.07	1.00	
Ag^+	1.15	1.03±0.05	1.60	[74]
Cl^-	1.81	1.74±0.05	1.00	
Ag^+	1.15	1.13	1.60	[75]
Br^-	1.46	1.76	1.15	
Mg^{2+}	0.72	0.90	1.50	[76]
F^-	1.33	1.25	0.50	

The idea of the continuous variation of the effective atomic size as the character of the chemical bond is varied between two limiting values—the ionic radius for the limiting ionic bond and the covalent radius for the covalent bond—is permissible. A linear variation of the radius with the amount of the ionic character of the chemical bond has been postulated. It was later shown that the variation of the dimensions of the electron shells (the so-called orbital radii) with the charge is not strictly linear.[73] Having adopted this model, one must not forget that the atomic and ionic radii are of a completely different character; the former are characterised by the distance from the centre of the atom to the maximum electron density of the valence electrons or, since these maxima overlap on formation of the chemical bond, to the maximum density of the electron overlap between the atoms, while the ionic radii are equal to the distance to the electron density minimum in the direction of the bonds between the atoms.

The dependence of the size of the atom on the effective charge can be regarded as semiempirical. For example, for silicon it can be described by the simple expression $r = r_k - 0.05Z^2$, where r_k is the covalent radius and Z the atomic charge. The theoretical values of the orbital radii of Si^+ (1.08 Å) and Si^{2+} (0.90 Å) are distributed between the covalent (1.16 Å) and ionic (0.40 Å for a coordination number of 6) radii.[24] It is important to emphasise that the average experimental radius of the silicon ion (0.96 Å), found for silicates, corresponds to a charge of +1.5 e. In its turn the estimated effective charge on the silicon atom agrees closely with the results of the analysis of the distribution of the electron density of silicon discussed above and with numerous data obtained by other physical methods.

Thus the description of the atom as a spherical body for significantly covalent compounds greatly simplifies the radial picture of chemical bonds. The study of the distribution of electron density in various polymorphic modifications of SiO_2 is extremely instructive in this sense. In the SiO_2 crystal with the rutile structure (stishovite),[77] the chains of SiO_2 octahedra having common edges are arranged along the c axis. Each chain is linked to four other chains via oxygen

atoms. It follows from the ionic model that the Si–Si and O–O repulsion in stishovite should lead to a longer Si–O bond directed along the common edge of the octahedra.[77] Experiment has shown that the deformation electron density peaks for the two bonds are respectively 0.47 and 0.30 eÅ^{-3} (Fig. 8*a*) and are somewhat displaced towards oxygen atoms. The distance from them to Si is 1.1 Å, which agrees fairly well with the Slater atomic radius of silicon.[78] The Si–O bonds in the four-membered ring are strained, which is indicated by the shift of the peaks to the outside from the line of the bond (Fig. 8*b*). It is striking that in this plane the peaks are linked by bridges; such distribution of deformation electron density is apparently preferable on energy grounds. In this case the electrons of the bridges shield the nuclei of the cations interacting via the common edge and for this reason, contrary to the ionic model, the corresponding Si–O bonds are shorter.

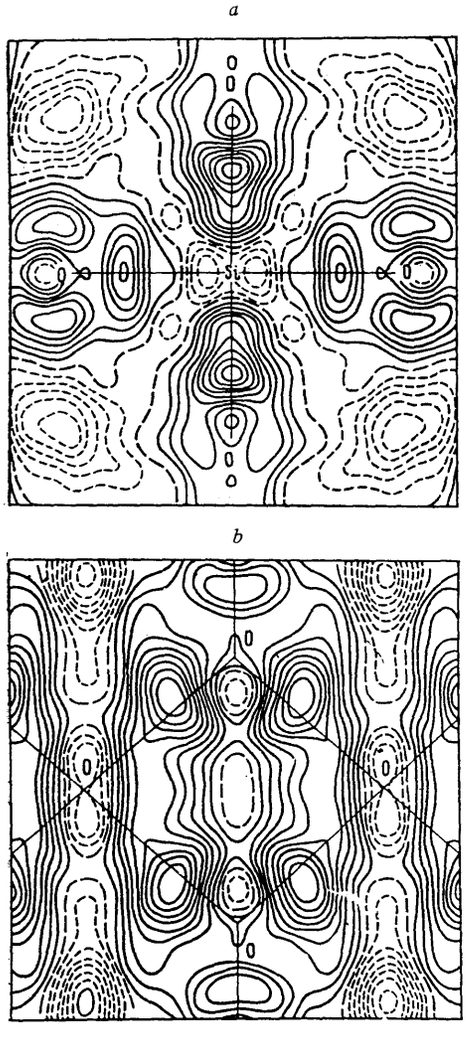


Figure 8. Deformation electron density in the stishovite (SiO_2) crystal:[72] *a*) section illustrating the non-equivalent Si–O bonds (the Si atom is in the centre); *b*) section through a four-membered ring made up of O atoms; the contour lines are drawn at 0.05 eÅ^{-3} intervals.

As in stishovite, the deformation electron density peaks have been found from the Si–O bonds in α- and β-quartz to one side of the line connecting the atoms.[79] In these SiO_2 modifications the deformation of the electron cloud is more complex. We may note the appreciable delocalisation of the electrons along the O–Si–O fragment and the displacement of the centres of gravity of the covalent peaks towards the oxygen atoms. Individual bonds are also linked by bridges, which may be interpreted as evidence for partial double bond character of the Si–O bond. Estimation of the atomic charges by the least squares method using the multipolar expansion showed that the effective charge on silicon in various SiO_2 modifications is in the range 1.0–1.7 e, while the charge on oxygen is between −0.5 and −0.85 e.[28] The charge on silicon with a coordination number (C.N.) of 4 is close to 1.0 e and for C.N. = 6 in stishovite it increases to 1.7 e. This indicates an increase of the amount of ionic character of the Si–O bond with increasing C.N. Using the parameter κ, it has been found that the silicon atom in the crystal has contracted while the oxygen atom has expanded relative to the dimensions of the free atoms.

A correlation has been observed experimentally in recent times between the charge on the silicon atom and its coordination number. In particular, it has been found for the compound $K_2Si^{VI}Si_3^{IV}O_9$, where the silicon atoms occupy both tetrahedral and octahedral positions,[80] that the charge on silicon increases with increasing C.N. Refinement of the populations of the valence shells yielded the charges +3.29(15) e for Si^{VI} and +2.52(11) e for Si^{IV}, which can be interpreted as an indication of an increase in the amount of ionic character of the bonds in which a Si atom participates as the coordination number of atoms increases.

Estimation of the atomic charges is the simplest method for finding an approximation to the experimental electron distribution. For this purpose, one usually employs either numerical integration of the electron density (for example, for cations over the volume of a sphere whose radius is equal to the radius of optimum separation[27]) or the refinement of the valence electron population of the atoms (as a rule with the aid of the κ technique[18] by the method of least squares). Both methods suffer from a series of disadvantages. Thus the result of the integration depends on the selected volume and that of the refinement procedure on the functions with the aid of which one calculates the scattering amplitude for the valence electrons. Furthermore, the data obtained by these methods agree poorly with one another (Table 6).[81] The estimated values for transition metal atoms in various coordination compounds quoted in Table 6 approach the formal oxidation state only in oxides and silicates (ionic crystals). In organometallic compounds they are appreciably below the formal oxidation states owing to the significant covalent contribution of the metal–ligand bonds. Thus the above estimated charges can hardly be regarded as characteristic of the valence state of the central atom in coordination compounds. More detailed information can be derived from the maps, which make it possible to identify the characteristics of the electronic structure of metal atoms in various crystals.

The study of dinuclear transition metal complexes is of great interest. The character of the chemical bond between the transition metal ions is in this case strikingly different both from the simple picture observed in covalent bonds involving light atoms without d electrons and from the metal–ligand bond. The observed large difference between the lengths of the quadruple M–M bonds (approximately 0.7 Å) shows that the distribution of electron density in various compounds containing such bonds can have significantly different details. The extensive experimental and theoretical studies proved useful for the understanding of the specific

features of these details. The dihydrate of dichromium tetra-acetate $Cr_2(O_2C_2H_3)_4.2H_2O$ has been investigated.[82] In this crystal the moelcule is located at the crystallographic centre of inversion and has an intrinsic D_{4h} symmetry. This made it possible to obtain fairly accurate results by averaging the experimental $\delta\rho$ maps over the chemically equivalent parts of the molecule. According to classical views, a quadruple metal–metal bond is formed in this compound, where the distance between the chromium atoms is 2.36 Å: a single σ-bond (described by the d_{z^2} orbital), two equivalent π-bonds (d_{xz} and d_{yz}), and a single weak δ-bond (d_{xy}) are formed. The contributions of each component differ very greatly in magnitude and the bond order indicated above therefore merely reflects the fact that it can be formally described by four molecular orbitals occupied by eight electrons. The experimental data (Fig. 9) show that the deformation electron density in the region of the metal–metal σ-bond is diffuse and significantly smaller in magnitude than in the Cr–O, C–O, and C–H bonds (approximately 0.1 eÅ^{-3} to within 0.02 eÅ^{-3}); on the other hand, somewhat higher peaks (0.12–0.3 eÅ^{-3}) are manifested in the region of π- and δ-bonds. These data agree well with theoretical calculations of the deformation electron density functions for $Cr_2(HCO_2)_4$ in terms of an expanded basis set taking into account configuration interaction.[82] Comparison of the electron populations of the 3*d* orbitals of the free chromium atom (spherically averaged) and the chromium atom in a molecule has shown that the population of the d_{z^2} orbital forming a σ-bond changes very insignificantly on formation of a molecule and the peaks in the corresponding region are therefore small. The more appreciable change in the populations of other orbitals is accompanied by the appearance of peaks far from the line of the bond. One should note that the 4*s* valence orbital in the molecule is almost unoccupied and this also entails a decrease of the deformation electron density between the metal atoms.

Table 6. Charges on transition metal atoms estimated from diffraction data.[81]

Atom	Atomic charge, e		Oxidation state	Compound
	I	II		
Co	+0.7 (1)	+0.06 (6)	+3	$[Co(NO_2)_6]^{3-}$
Co	+0.7 (3)	+0.8 (1)	+3	$[Co(NH_3)_6]^{3+}$
Co	+0.2 (3)	+0.4 (1)	+3	$[Co(CN)_6]^{3-}$
Cr	+0.15 (12)	—	0	$[Cr(Co)_6]$
Cr	+0.1 (1)	+2.78 (6)	+6	CrO_4^{2-}
Co	—	+1.5 (1)	+2	$CoAl_2O_4$
Mn	+1.58 (1)	—	+2	MnO
Mn	+0.21 (6), +1.49 (6)	—	+2	Mn_2SiO_4
Fe	+0.85 (8), +1.54 (7)	+1.3 (1), +1.9 (1)	+2	α-Fe_2SiO_4
Mn	+1.21 (6), +1.49 (6)	+1.3 (1), +2.2 (2)	+2	α-Mn_2SiO_4

Remarks: The charges quoted in column I were found by the numerical integration of the electron density within the limits of the sphere defined by the optimum separation radius, while column II lists the charges found by the κ-refinement using the method of least squares.

When configuration interaction was taken into account, it was found[82] that the $\sigma^2\delta^2(\delta^*)^2(\sigma^*)^2$ configuration makes a considerable contribution to the energy of the structure; the contribution of the highly bonding $\sigma^2\pi^4\delta^2$ configuration is only 18%. Thus the antibonding configurations diminish with formal bond order, increasing the bond length.

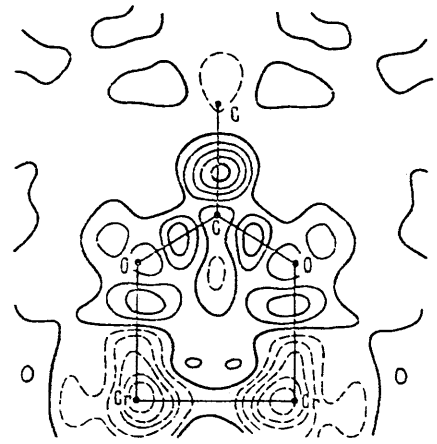


Figure 9. Experimental map of the deformation electron density in the $Cr_2(O_2C_2H_3)_4.2H_2O$ crystal; the section containing the Cr–Cr bond is shown; spacing between lines 0.1 eÅ^{-3}.

The characteristic features of the $\delta\rho$ map in $Mo_2(O_2C_2H_3)_4$ in the region of the Mo–Mo bond, whose length is 2.10 Å, are qualitatively similar to the picture described above. However, more intense peaks have been observed[83] between the metal atoms (approximately 0.2 eÅ^{-3}) also to one side of the Mo–Mo line (approximately 0.4 eÅ^{-3}). Calculated data for the changes in the electron populations of molybdenum[83] suggest that the explanation of the causes of the increase of $\delta\rho$ in the region of the π- and δ-bonds adduced above in connection with the consideration of $Cr_2(O_2C_2H_3)_4.2H_2O$ is valid also in the case under discussion. Next it was found for $Mo_2(O_2C_2H_3)_4$ that the transfer of electrons from Mo to the neighbouring atoms is accompanied by the appearance of negative minima in the vicinity of the Mo atom on the $\delta\rho$ map in directions corresponding to a decrease of electron density in the antibonding $d_{x^2-y^2}$ orbital. This is characteristic of a transition metal ion in a crystal field with D_{4h} symmetry. It is noteworthy that, in contrast to $Cr_2(O_2C_2H_3)_4.2H_2O$, the contribution of the configuration of the ground state $\sigma^2\pi^4\delta^2$ in this compound is 66% and allowance for the excited configuration hardly alters the deformation electron density map.

The refined features of the electron density in the "ultrashort" quaternary Cr–Cr bond in $[Cr_2(mhp)_4]$, whose length is 1.879 Å at 74 K, have been studied in detail.[84]¶ A $\delta\rho$ peak 0.41 eÅ^{-3} high, extending over the π- and δ-regions, has been observed between the metal atoms (Fig. 10*a*). This peak is so diffuse that it is linked by $\delta\rho$ bridges 0.15 eÅ^{-3} high with the peaks on the metal–ligand

¶ Here mhp = μ-2-hydroxy-6-methylpyridine.

bond. Quantum-chemical calculation for the $Cr_2[H_2P(CH_2)_2]_4$ molecule has shown[84] that the contribution of the δ-component to such a quadruple bond is relatively small and that the σ- and π-interactions play the main role. Negative δρ regions approximately -0.37 eÅ^{-3} deep are directed towards the ligand; this indicates a smaller electron population of the $d_{x^2-y^2}$ orbital compared with the d_{xy} orbital. This is why the $d_{x^2-y^2}$ orbital in fact serves as an acceptor for the unshared electron pairs of the ligands, promoting the formation of a donor–acceptor bond. The theoretical δρ map (Fig.10*b*), calculated taking into account configuration interaction (the contribution of the $\sigma^2\pi^4\delta^2$ configuration is 55%), agrees well with the experimental map: for example, the height of the peak on the M–M bond is in this case 0.30 eA^{-3}. Excess density peaks are observed in both cases when the line of this bond is produced (0.3–0.45 eÅ^{-3}), which is caused, according to the authors,[84] by the contraction of the 3*p* and 3*s* shells. Such peaks have also been observed for $Mo_2(O_2C_2R_3)_4$, but could not be interpreted reliably.

Thus experiment has shown that formally identical quadruple metal–metal chemical bonds have, apart from common features, all the characteristic features associated with the specific composition and structure of the compound. This conclusion has been confirmed and supplemented by theoretical calculations. Thus the cases discussed above indicate a tendency towards an increase of the δρ peak located between the metal atoms with decrease of the bond length. On the other hand, the observed small population of the $d_{x^2-y^2}$ orbital changes from compound to compound depending on the nature of the metal atoms and the type of ligand, which alters the ligand–metal–metal angle, changing at the same time the geometry of the compound as a whole. Allowance for the interelectron interaction in binary complexes, which significantly reduces the energy of the system, has different effects on the deformation electron density in various compounds, sometimes leading merely to changes in insignificant details.

In interpreting the deformation electron density maps, one should bear in mind that the construction of difference electron density maps always involves an arbitrary element, because they depend on the choice of the model of the promolecule,[85] which can be made up, in principle, of the electron densities of the free atoms or spherically averaged atoms forming part of the molecule. In the former case the atoms with incompletely occupied *p* and *d* shells have non-zero angular moments and possess a characteristic symmetry. As a consequence of this, differences arise between the electron densities along the chemical bond and at right angles to it and are manifested on the δρ maps. In particular,[85] if the B and C atoms in the ground state are included in the promolecule, then the values of the δρ function along the line of the bond are smaller than in the case where the electron densities of these atoms are spherically averaged. The opposite picture is observed for O and F atoms. For this reason, it is recommended[85] that the promolecule be defined as the set of the electron densities of spherically symmetrical atoms; this reference state has since become generally adopted.

In the calculation of the valence electron density, the separation of electrons into "inner" and "outer" is usually carried out on the grounds of energy considerations. It is then assumed that the densities (and energies) of the "inner" electrons in the molecules and in the free atoms are virtually the same. However, it is known from calculations that, when atoms are involved in a chemical bond, the energies of the inner shells change somewhat.[86] This is also indicated by photoelectron spectroscopic data.[87] Another deficiency of the energy approach to the separation consists in the fact that is is not clear how it can be applied to the electrons of the *s* orbitals located not only in the valence region but also in the vicinity of atomic nuclei.

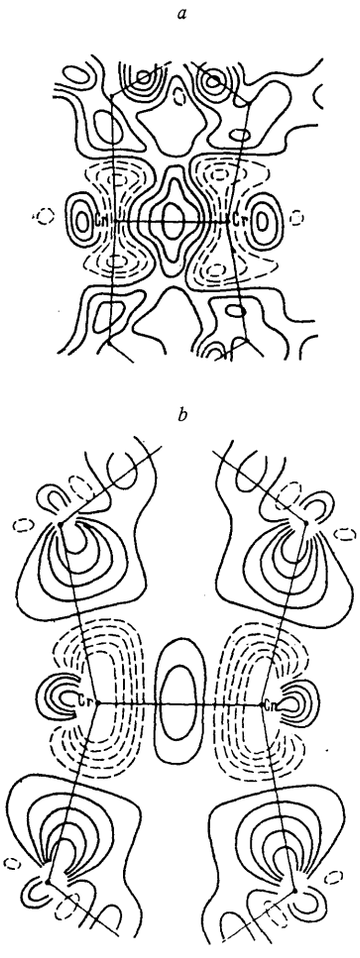


Figure 10. Experimental (*a*) and theoretical (*b*) maps of the deformation electron density in the "ultrashort" quadruple Cr–Cr bond;[84] spacing between lines 0.1 eÅ^{-3}.

At the same time, it has been noted[88] that points where the radial distribution of the electron density has local minima, whose number is equal to the number of nodes in the radial wave function, exist in atoms. It has been suggested[89] that these minima be regarded as the boundaries between the *K*, *L*, ... layers in the electron shells of atoms. This provides a natural criterion for the subdivision of electrons into skeletal and valence electrons. In molecules the spherical symmetry of the atom breaks down and its electron skeleton is polarised: the skeleton contracts along the bond and expands in a perpendicular direction (dipolar polarisation).[90] However, this polarisation is relatively insensitive to the nature of the other atoms involved in the

chemical bond and the above definition of the skeleton is therefore very suitable for the identification of valence electrons.

Careful analysis[21] made it possible to elucidate the role of the nodes in wave functions in the formation of a chemical bond. An increase of their number in σ orbitals weakens the role of the σ-electron density in the formation of chemical bonds; at the same time the contribution to the electron density described by the π, δ, and other orbitals increases. For this reason, the covalent bonds involving the C, N, and O bonds are apparently stronger than the bonds involving the Si, P, and S atoms.[21]

On the basis of the foregoing, one can conclude that positive peaks on the δρ maps will be manifested in the bonding and non-bonding regions of the molecule and the crystal, while the negative peaks will occur in the regions where the atomic orbitals whose contribution to the molecular orbitals are small are localised. Comparison of the spatial characteristics of the atomic orbitals with the observed electron distribution permits a qualitative interpretation of the latter in terms of the LCAO-MO approximation. Here it is essential to note that the absence of positive δρ peaks in the bonding region does not indicate the absence of a covalent bond. For example, we can imagine a molecular orbital, describing the region of the bond, in the form of a linear combination of the hybrid orbitals of atoms in close proximity each of which supplies one electron to the bond. If these atoms contain more than half-occupied valence shells, then, after spherical averaging, there will be more than one electron per hybrid atomic orbital. In the calculation of the δρ function, this cannot only compensate for the corresponding peaks but can also lead to their negative values in the region of the bond.

Indeed the results of the experimental and theoretical studies have confirmed these considerations. The above picture has been observed, for example, in the N–N bond of diformylhydrazide,[91] the O–O bond in hydrogen peroxide,[92] the C–F bond in tetrafluoroterephthalodinitrile,[93] and also in certain M–M bonds discussed above. We may note the choice of the reference state in a form different from the promolecule (see, for example, Heijser et al.[94]) makes it possible to identify the characteristics of the distribution of the deformation electron density also in such cases, which are difficult to interpret by the standard procedure.

The above refers also to the regions where the unshared electron pairs are located, their peak diminishing and being observed nearer to the centres of the atoms with increase of the electronegativity of the latter.[93] Thus, in the interpretation of the deformation electron density maps, one must take into account the distribution of electrons among the orbitals in the atoms of the promolecule averaged over the orientations.

---o0o---

It is seen from the data presented that modern diffraction methods make it possible to obtain a clear and detailed picture of the structures of crystalline substances which had been inaccessible hitherto. The new data sometimes agree with the existing crystal-chemical and quantum-chemical views, supplementing and refining them, and sometimes contradict them. At the present time experimental data for a wide range of systems are accumulating rapidly. The electron densities in the fragments of complex biological molecules, medicinal drugs, the organometallic compounds involved in catalytic processes, substances used in instrument making, and minerals are being investigated. A general treatment of these data will enable us to move from qualitative correlations to the establishment of quantitative relations between the electronic structures of substances and their physicochemical properties. So far only the first attempts have been made to seek such relations in the solution of problems concerning complex formation[95] and in the study of materials for non-linear optics;[96] a further development of this approach appears extremely promising.

REFERENCES

1. P.Becker (Editor), "Electron and Magnetisation Density in Molecules and Crystals", Plenum Press, New York, 1980, p.915.
2. R.McWeeny and B.T.Sutcliffe, "Methods of Molecular Quantum Mechanics" (Translated into Russian), Izd. Mir, Moscow, 1972, p.380.
3. K.Ohno and K.Morokuma (Editors), "Quantum Chemistry Literature Data Base", New York, 1981.
4. G.De With and D.Feil, Chem.Phys.Letters, 1975, **30**, 279.
5. P.Becker, Phys.Scripta, 1977, **15**, 119.
6. B.K.Vainshtein, "Sovremennaya Kristallografiya" (Modern Crystallography), Izd.Nauka, Moscow, 1979, Vol.1, p.383.
7. "International Tables for X-Ray Crystallography", Kynoch Press, Birmingham, Vol.4, 1974.
8. B.T.M.Willis and A.W.Pryor, "Thermal Vibration in Crystallography", University Press, Cambridge, 1975.
9. Yu.Z.Nozik, R.P.Ozerov, and K.Hennig, "Strukturnaya Neitronografiya" (Structural Neutron Diffraction), Atomizdat, Moscow, 1979, p.343.
10. I.V.Voloshina, V.G.Tsirel'son, V.S.Arutyunov, and R.P.Ozerov, Kristallografiya, 1984, **29**, 864.
11. D.M.Kheiker, "Rentgenovskaya Difraktometriya Monokristallov" (X-Ray Diffractometry of Single Crystals), Izd.Mashinostroenie, Moscow, 1973, p.255.
12. P.Coppens, in "Neutron Diffraction" (Edited by H.Dachs), Springer Verlag, New York, 1978, p.71.
13. P.Becker and P.Coppens, Acta Cryst., 1974, **A30**, 129.
14. G.H.Ramachandran and R.Srivansan (Editors), "Fourier Method in Crystallography", International Union of Crystallography Publ., Copenhagen, 1970.
15. D.T.Cromer and D.Liberman, J.Chem.Phys., 1970, **53**, 1891.
16. V.G.Tsirel'son, E.V.Parini, and R.P.Ozerov, Dokl. Akad.Nauk SSSR, 1980, **254**, 370.
17. R.F.Stewart, J.Chem.Phys., 1968, **48**, 4882.
18. P.Coppens, T.N.Guru Row, P.Leung, E.D.Stevens, P.Becker, and Y.W.Yang, Acta Cryst., 1979, **A35**, 63.
19. H.Hansen and P.Coppens, Acta Cryst., 1978, **34**, 909.

20. F.L.Hirshfeld, Acta Cryst., 1976, **A32**, 239.
21. F.L.Hirshfeld and S.Rzotkiewicz, Mol.Phys., 1974, **27**, 1319.
22. V.G.Tsirel'son, M.Yu.Antipin, R.G.Gerr, R.P.Ozerov, and Yu.T.Struchkov, Phys.Stat.Solidi, 1985, **A87**, 425.
23. V.G.Tsirel'son and R.P.Ozerov, in "Difraktsionnye Metody Issledovaniya Veshchestva" (Diffraction Methods for the Study of Matter), Izd.Shtiintsa, Kishinev, 1981, p.47.
24. V.G.Tsirel'son, Yu.Z.Nozik, and V.S.Urusuov, Geokhimiya, 1984, (2), 160.
25. B.Rees, Acta Cryst., 1976, **A32**, 483.
26. V.G.Tsirel'son and Yu.Z.Nozik, Kristallografiya, 1982, **27**, 863.
27. S.Sasaki, K.Fujino, Y.Takeuchi, and R.Sadanaga, Acta Cryst., 1980, **A36**, 904.
28. S.Sasaki, V.Takeuchi, K.Fujino, and S.Z.Akimoto, Krist., 1982, **158**, 279.
29. R.F.Stewart, J.Chem.Phys., 1970, **53**, 205.
30. F.L.Hirshfeld, Acta Cryst., 1971, **B27**, 769.
31. M.Harel and F.L.Hirshfeld, Acta Cryst., 1975, **B31**, 162.
32. R.F.Stewart, Acta Cryst., 1976, **A32**, 565.
33. A.Holladay, P.Leung, and P.Coppens, Acta Cryst., 1983, **A39**, 377.
34. E.D.Stevens, J.Amer.Chem.Soc., 1981, **103**, 5087.
35. D.Schwarzenbach and Ngo Thong, Acta Cryst., 1979, **A35**, 652.
36. R.F.Stewart, J.Cher.Phys., 1973, **58**, 1668.
37. R.Chen, P.Trucano, and R.F.Stewart, Acta Cryst., 1977, **A33**, 823.
38. W.J.Hehre, R.Ditchfield, R.F.Stewart, and J.A.Pople, J.Chem.Phys., **52**, 2769.
39. P.Coppens, D.Pautler, and J.F.Griffin, J.Amer. Chem.Soc., 1971, **93**, 1051.
40. P.Coppens, T.V.Willoughby, and L.N.Csonka, Acta Cryst., 1971, **A27**, 248.
41. R.H.O'Connor and E.N.Maslen, Acta Cryst., 1974, **B30**, 383.
42. D.S.Jones, D.Pautler, and P.Coppens, Acta Cryst., 1972, **A28**, 635.
43. A.J.Allen-Williams, A.J.Delaney, R.Furina, E.N.Maslen, B.H.O'Conner, J.V.Varghese, and Young Fook Hong, Acta Cryst., 1975, **A31**, 101.
44. V.G.Tsirel'son and R.P.Ozerov, Zhur.Strukt.Khim., 1978, **19**, 558.
45. W.L.Clinton and L.J.Massa, Phys.Rev.Letters, 1972, **29**, 1363.
46. W.L.Clinton, C.A.Frishberg, L.J.Massa, and P.A.Oldfield, Int.J.Quant.Chem.Symp., 1973, **7**, 505.
47. V.G.Tsirel'son, M.M.Mestechkin, and R.P.Ozerov, Dokl.Akad.Nauk SSSR, 1977, **233**, 108.
48. C.A.Frisnberg and L.J.Massa, Int.J.Quantum.Chem. Symp., 1978, **13**, 801.
49. V.G.Tsirel'son, V.E.Zavodnik, E.B.Fomicheva, R.P.Ozerov, L.I.Kuznetsova, and I.S.Rez, Kristallografiya, 1980, **25**, 735.
50. V.G.Tsirel'son, L.N.Kuleshova, and R.P.Ozerov, Kristallografiya, 1981, **26**, 1312.
51. E.Scrocco and J.Tomasi, Adv.Quant.Chem., 1978, **12**, 115.
52. A.A.Varnek, V.G.Tsirel'son, and R.P.Ozerov, Dokl. Akad.Nauk SSSR, 1981, **257**, 382.
53. M.Spackmann and R.F.Stewart, in "Chemical Applications of Atomic and Molecular Electrostatic Potentials" (Edited by P.Polizer and D.Truhlar), Plenum Press, New York, 1981, p.407.
54. J.Epstein and D.J.Swanton, J.Chem.Phys., 1982, **77**, 1048.
55. P.Hohenberg and W.Kohn, Phys.Rev., 1964, **136**, 864.
56. J.Katriel, J.Phys.C, Solid State Phys., 1980, **13**, L375.
57. J.Riess and W.Münch, Theor.Chem.Acta, 1981, **58**, 295.
58. D.P.Murphy and W.F.Wang, J.Chem.Phys., 1980, **72**, 429.
59. P.Politzer and R.Parr, J.Chem.Phys., 1974, **11**, 4258.
60. J.Bentley, J.Chem.Phys., 1979, **70**, 159.
61. B.T.M.Willis, Acta Cryst., 1969, **A25**, 277.
62. C.Kittel, "Introduction to Solid State Physics" (Translated into Russian), Izd.Nauka, Moscow, 1978.
63. G.G.Gel'man, "Kvantovaya Khimiya" (Quantum Chemistry), ONTI, Moscow, 1937.
64. R.Feynman, Phys.Rev., 1939, **59**, 340.
65. U.H.Zucker and H.Schulz, Acta Cryst., 1982, **A38**, 563.
66. H.Schulz, in "The Physics of Super-Ionic Conductors and Electrode Materials"(Edited by J.W.Perram), Plenum Press, New York, 1983, p.3.
67. U.H.Zucker and H.Schulz, Acta Cryst., 1982, **A38**, 568.
68. U.van Alpern, U.Rabenau, and G.H.Talat, Appl. Phys.Letters, 1977, **30**, 621.
69. K.Tanaka and F.Marumo, Acta Cryst., 1982, **B28**, 1422.
70. A.Gavezzotti and M.Simonetta, Chem.Phys., 1982, **82**, 1.
71. V.G.Tsirel'son, Symposium, "Elektronnoe Sostoyanie Molekul i Khimicheskaya Svyaz'. Trudy MKhTI" (The Electronic Structure of Molecules and the Chemical Bond. Transactions of the Moscow Institute of Chemical Engineering), Moscow, 1984, No.134, p.37.
72. N.N.Lobanov, V.G.Tsirel'son, and R.P.Ozerov, Solid State Comm., 1984, **50**, 129.
73. V.S.Urusov, "Energeticheskaya Kristallokhimiya" (Energetic Crystal Chemistry), Izd.Nauka, Moscow, 1975.
74. M.V.Linkoaho, Acta Cryst., 1969, **A25**, 450.
75. E.Vogl and W.Waidelich, Z.angew.Phys., 1968, **25**, 98.
76. J.Vidal, G.Vidal-Valat, M.Gaitler, and K.Kurki-Suonio, Acta Cryst., 1981, **A37**, 826.
77. R.J.Hill, M.D.Newton, and G.V.Gibbs, J.Solid State Chem., 1983, **47**, 185.
78. J.C.Slater, J.Chem.Phys., 1964, **41**, 3199.
79. D.Schwarzenbach and Ngo Thong, in "Abstracts of the European Crystallographic Meeting, Copenhagen, 1979", p.348.
80. D.K.Swanson and C.T.Prewitt, American Mineralogist, 1983, **68**, 581.
81. K.Toriumi and Y.Saito, Adv.Inorg.Chem.Radiochem., 1983, **27**, 27.
82. M.Benard, P.Coppens, M.L.De Lucia, and E.D.Stevens, Inorg.Chem., 1980, **19**, 1924.
83. K.Hino, Y.Saito, and M.Benard, Acta Cryst., 1981, **B37**, 2164.
84. A.Mitschler, B.Rees, R.Wiest, and M.Benard, J.Amer. Chem.Soc., 1982, **104**, 7501.
85. B.J.Ransil, J.J.Sinai, J.Amer.Chem.Soc., 1972, **94**, 7268.
86. J.J.Bentley and R.F.Stewart, Acta Cryst., 1974, **A30**, 60.
87. W.Jolley and A.Bakke, in "Electron Distribution and the Chemical Bond" (Edited by P.Coppens and M.B.Hall), Plenum Press, New York, 1982, p.431.

88. H.Weinstein, P.Politzer, and S.Srebrenik, Theor. Chim.Acta, 1975, **38**, 159.
89. P.Politzer and R.G.Parr, J.Chem.Phys., 1976, **64**, 4634.
90. P.Politzer, J.Reuther, and G.T.Kasten, J.Chem. Phys., 1976, **67**, 2385.
91. T.Ottersen, J.Almlöf, and H.Hope, Acta Cryst., 1980, **B36**, 1147.
92. J.M.Savariault and M.S.Lehmann, J.Amer.Chem. Soc., 1980, **102**, 1298.
93. J.D.Dunitz, W.B.Schweizer, and P.Seiler, Helv. Chim.Acta, 1983, **66**, 123.
94. W.Heijser, E.J.Baerends, and P.Ros, J.Chem.Soc., Faraday Discuss., 1980, **14**, 211.
95. O.M.Petrukhin, A.A.Varnek, R.P.Ozerov, V.G.Tsirel'son, and G.A.Yagodin, "Trudy MKhTI" (Transactions of the Moscow Institute of Chemical Engineering), Moscow, 1984, No.134, p.87.
96. V.G.Tsirel'son, O.V.Korol'kova, R.P.Ozerov, and I.S.Rez, Phys.Stat.Solidi, 1984, **122**(B), 599.

Mendeleev Moscow Institute of
Chemical Engineering

Vernadskii Institute of Geochemistry
and Analytical Chemistry,
USSR Academy of Sciences,
Moscow